ELSEVIER

International Journal of Minerals, Metallurgy and Materials
Volume 16, Number 4, August 2009, Page 444

Materials

Effect of nano-SiC particles on the corrosion resistance of NiP-SiC composite coatings

Xue-tao Yuan[1)], *Dong-bai Sun*[1,2)], *Hong-ying Yu*[1,2)], *and Yu Wang*[1)]

1) School of Materials Science and Technology, University of Science and Technology Beijing, Beijing 100083, China
2) Beijing Engineering-Research Center for Surface Nano-Technology, Beijing 100083, China
(Received 2008-06-20)

Abstract: NiP-SiC (≈11wt% P) composite coatings were electroplated in a Brenner type plating bath. The coatings had amorphous nano-phase composite structure. Direct current and alternating current electrochemical tests were carried out on such coatings in a 3.5wt% solution of NaCl to evaluate their corrosion resistance. The potentiodynamic polarization, electrochemical impedance spectroscopy (EIS) tests, and exposure experiments all show that the corrosion resistance of NiP-SiC coatings first increases and then decreases when the SiC content increases, but the corrosion resistance of NiP-SiC composite coating is better than that of amorphous NiP coatings.

Key words: electroplating; composite coating; nanoparticle; corrosion resistance; electrochemical impedance spectroscopy

[*This work was financially supported by the National High-Tech Research and Development Program of China (No.2002AA331080) and the Scientific Research Key Program of Beijing Municipal Commission of Education (No.KZ200410028012).*]

1. Introduction

The nickel-phosphorus (Ni-P) coating is widely used in different industries because of its excellent corrosion and wear resistances [1-2]. Moreover, it is known that the incorporation of particles into this NiP matrix provides enhanced surface properties, depending on the particle nature [3]. Hard particle-containing coatings (NiP/*X*, *X*=SiC, WC, Al_2O_3, Si_3N_4, *etc.*) have been developed when the main requirement for a composite coating is wear resistance [4-5]. Among these coatings, the NiP-SiC composite coating has been proved to be the most cost-effective and best-performing combination [5]. While maintaining the original good performance of a NiP coating, its wear resistance has been substantially improved, several times or even several tens of times better than that of a hard chromium coating [6]; therefore, it has broader application. The final properties of NiP-SiC coatings depend on the phosphorus content of the NiP matrix which determines the structure of coatings, and on the characteristics of embedded particles such as type, shape and size. In recent researches, most studies concerning NiP-hard particle systems are performed using micron-sized particles. Because the granularity of particles is large, particles are not uniformly distributed on the NiP coating, the potential performance of the composite coating has not yet been fully developed. However, in recent years, nano-technology has been developed rapidly, metal-based nano-composite coatings have been received extensive attention for their unique performance.

Although there were reports about the study of nano-sized SiC particles in the NiP coating, most of them were about the influence of nano-SiC particulates on the wear resistance of the coating [7-14], very few were about influence of SiC particles on the corrosion resistance of the NiP coating. Study results of different researchers about the influence of nano-particles on the corrosion resistance of the composite coatings were different, even contradictory in many cases [15-16]. Therefore, further study in this field is of great theoretical and practical value, and this paper focuses on the effect of nano-SiC particles on the corrosion resistance of the NiP coating.

Corresponding author: Xue-tao Yuan, **E-mail:** nczhongya@163.com
Also available online at www.sciencedirect.com

2. Experimental

2.1. Preparation of NiP-SiC composite coatings

The composition of the basic bath used for the preparation of NiP-SiC composite electrodeposits with the P content around 11wt% is given in Table 1. The solutions were prepared from analytic grade chemicals and double distilled water. The pH value of the bath was measured by an HM-20E pH-meter and was adjusted to appropriate values with $NH_3 \cdot H_2O$ (25wt%) or/and H_2SO_4 (25wt%) solution. The electroplating bath temperature was maintained at 60±0.5°C by a water thermostat.

Table 1. Composition and operating conditions of the plating bath

Constituents of plating bath	Concentration / ($g \cdot L^{-1}$)
$NiSO_4 \cdot 6H_2O$	150.0
$NiCl_2 \cdot 6H_2O$	45.0
$NiCO_3 \cdot 2Ni(OH)_2 \cdot 4H_2O$	32.0
H_3PO_3	20.0
H_3PO_4	35.0
SiC	1.0-30.0
Dispersant agent	0.1

Operating conditions: pH=1.6; current density (i)=2 A/dm^2; temperature=60±1°C; plating time=90 min.

A pure copper sheet (15 mm×15 mm×0.1 mm) was used as a substrate, and a high purity (99.99%) electrolytic nickel plate was used as the soluble anode. Its surface area was approximately 10 times greater than that of the cathode to ensure that there were no problems arising from anode polarization, particularly at high current densities. The substrate was first chemically degreased, rinsed with distilled water, and then scrubbed with alcohol and acetone. The substrate was then acid-cleaned with a mixed solution of 16 mL H_2SO_4 (98wt%) and 50 mL HNO_3 (67wt%) in 1 L mixed solution for 5 s. The substrate was then activated with dilute H_2SO_4 (5wt%) for 30 s, and finally rinsed with pure water. After that, it was placed vertically in the electroplating cell of 0.5 dm^3 with magnetic stirring, parallel to the anode, with an anode-cathode distance of 5 cm. Every NiP-SiC coating was prepared in a fresh electroplating bath to avoid any complicated influences due to changes in concentration of the electroactive species.

2.2. Surface analysis

The chemical composition of coatings was determined by chemical titration, and the average values were adopted. Before and after electrochemical investigations, scanning electron microscope (SEM) (Cambridge S-360) was used to determine the surface morphology of the NiP/NiP-SiC coatings. The phase compositions of the as-deposited layer were examined with X-ray diffraction (XRD) (D/max-rB, RICOH, Japan) with a Cu K_α radiation (with λ=0.15406 nm). The diffraction patterns were analyzed using Jade5.0 software with the aid of JCPDS database. Transmission electron microscopy (TEM) investigations were carried out in Philips CM-12.

2.3. Electrochemical measurements

Electrochemical impedance spectroscopy (EIS) and potentiodynamic polarization measurements were performed using an Autolab PGSTAT30 galvanostat/potentiostat system. The measurements were performed using a conventional three-electrode cell, in which test sample (NiP/NiP-SiC coatings) was placed in Teflon sample holder and the exposed surface area to the corrosive medium was 1 cm^2. A saturated calomel electrode (SCE) and a platinum electrode of 6 cm^2 area were served as a reference and counter electrode, respectively. A Haber-Luggin capillary was placed in front of the work electrode. Potentiodynamic and impedance measurements of the NiP/NiP-SiC coatings were carried out in a 3.5wt% solution (pH=6) of NaCl at 25°C. Both potentiodynamic polarization and EIS measurements were performed in non-deaerated conditions.

(1) Electrochemical impedance spectroscopy

Impedance measurements were conducted using a frequency response analyzer. The EIS measurements were obtained by applying a sinusoidal perturbation of ±10 mV and the frequency range from 100 kHz to 10 mHz. The electrode potential for each sample was held at its stable open circuit potential (E_{ocp}) during EIS measurements. After each experiment the impedance data was displayed as Nyquist plots. A circuit description code (CDC) was assigned for the acquired data and the acquired data were curve fitted and analyzed using EQUIVCRT program [17].

(2) Potentiodynamic polarization

After EIS measurements, the system was allowed for some time to attain its stable E_{ocp}. The potentiodynamic polarization measurements were performed using the GPES program. The sweep rate was set at 1 mV/s and the potential was changed from cathode to anode values in a range of –250 mV to –450 mV. The corrosion potential (E_{corr}) and the corrosion current densities (i_{corr}) were determined using the Tafel extrapolation method [18].

3. Results and discussion

Different NiP-SiC specimens were prepared with different SiC concentrations (1-30 g/L). These speci-

mens were coded with the name of the NiP-SiC followed by their concentration. For example, the NiP-SiC specimen prepared in the solution containing 2 g/L of SiC was coded as NiP-SiC2. A reference specimen (NiP coating) was prepared without SiC.

The P content of the electrodeposits is shown as a function of SiC concentration in Fig. 1. The SiC concentrations used to produce specimens for corrosion testing were selected so that the difference in P content was insignificant (±0.5wt%) over the range studied. In Fig. 1, the phosphorus content in specimens NiP-SiC2, NiP-SiC5, and NiP-SiC10 are 10.90wt%, 10.64wt%, and 10.53wt%, respectively. Thus, with these three specimens, differences in the corrosion behaviour were unlikely to be attributable to differences in the P content of the coatings.

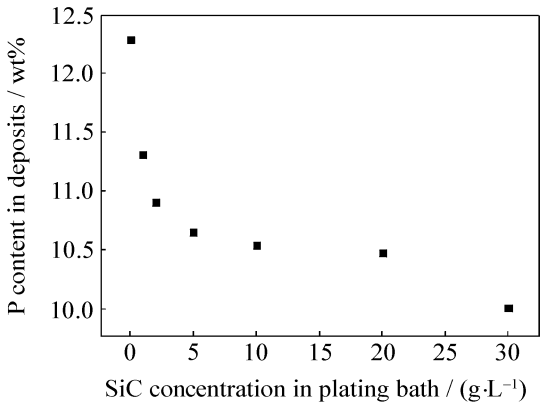

Fig. 1. Phosphorus contents related with SiC concentration in deposits in the plating bath.

3.1. Structure of NiP/NiP-SiC deposits

Previous to the co-deposition process, the SiC particles were characterized with respect to size and morphology. TEM images of the powders (Fig. 2) indicate that the SiC particles are polygonal, with a rather homogeneous size of about 50 nm.

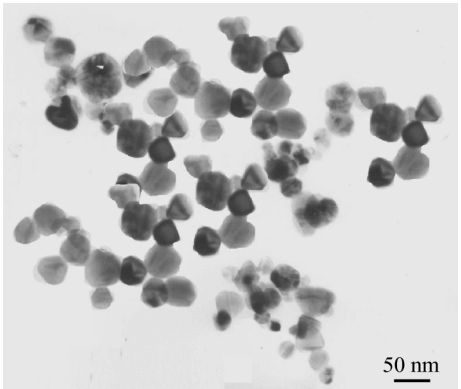

Fig. 2. Bright field TEM micrograph of SiC particles.

The diffraction patterns of as-deposited NiP and NiP-SiC10 coatings are shown in Fig. 3. It can be found that compared with the NiP coating, the diffraction pattern of the NiP-SiC10 composite coating has characteristic diffraction peaks of SiC.

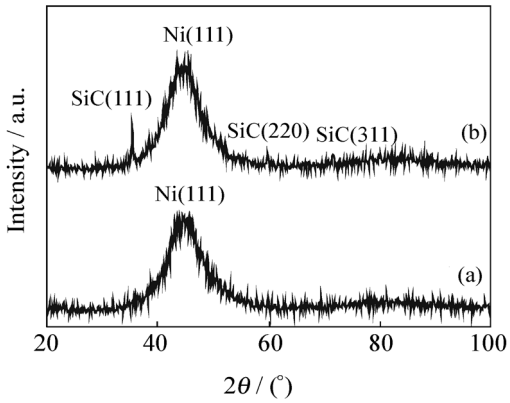

Fig. 3. XRD patterns of electroplating coatings: (a) NiP amorphous deposits; (b) NiP-SiC10 composite deposits.

Fig. 4 shows the TEM bright field image of the NiP-SiC10 composite coating. It can be seen that the nano-SiC particles are suspended in the NiP amorphous phase. The electron diffraction pattern of the NiP-SiC10 coating shows two types of diffraction rings, that is, amorphous-halo in the middle of the electron diffraction and very clear reflections. Thus, it can be said that this coating contains two types of phases. The amorphous-halo indicates the presence of amorphous NiP phase. The clear reflections from the electron diffraction pattern also indicate the presence of a phase containing large grains, which are indexed as a SiC compound with a face centered cubic (FCC) structure.

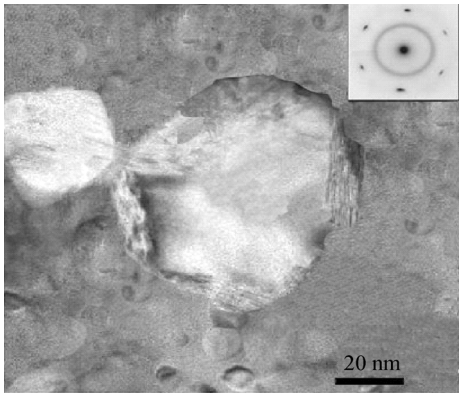

Fig. 4. Bright field TEM micrograph with an electron diffraction pattern of the NiP-SiC10 coating.

From the testing results of XRD and TEM, NiP-SiC coatings had amorphous-nanophase composite structure, that is to say, the inclusions of SiC particles introduced nanophase into the NiP coating, but could not change the amorphous structure of the NiP matrix in the electroplating process.

3.2. Surface morphology and composition

It can be seen from Figs. 5(a1)-(d2) and Table 2

that, with the increase in concentration of SiC particles in the bath, the content and the average particle size of SiC in NiP coatings increased gradually. When 2 or 5 g/L SiC particles were added into the bath, SiC particles were dispersed on amorphous coatings without obvious agglomerates. When SiC was increased to 10 g/L, although the compound quantity of SiC increased obviously, the average size of SiC particles in coating was about 700 nm. It was because with the increase of particle concentration, collision probability between SiC particles increased, then SiC particles accumulated on the coating surface and formed obvious agglomerates, and consequently appeared 'cauliflower' shape.

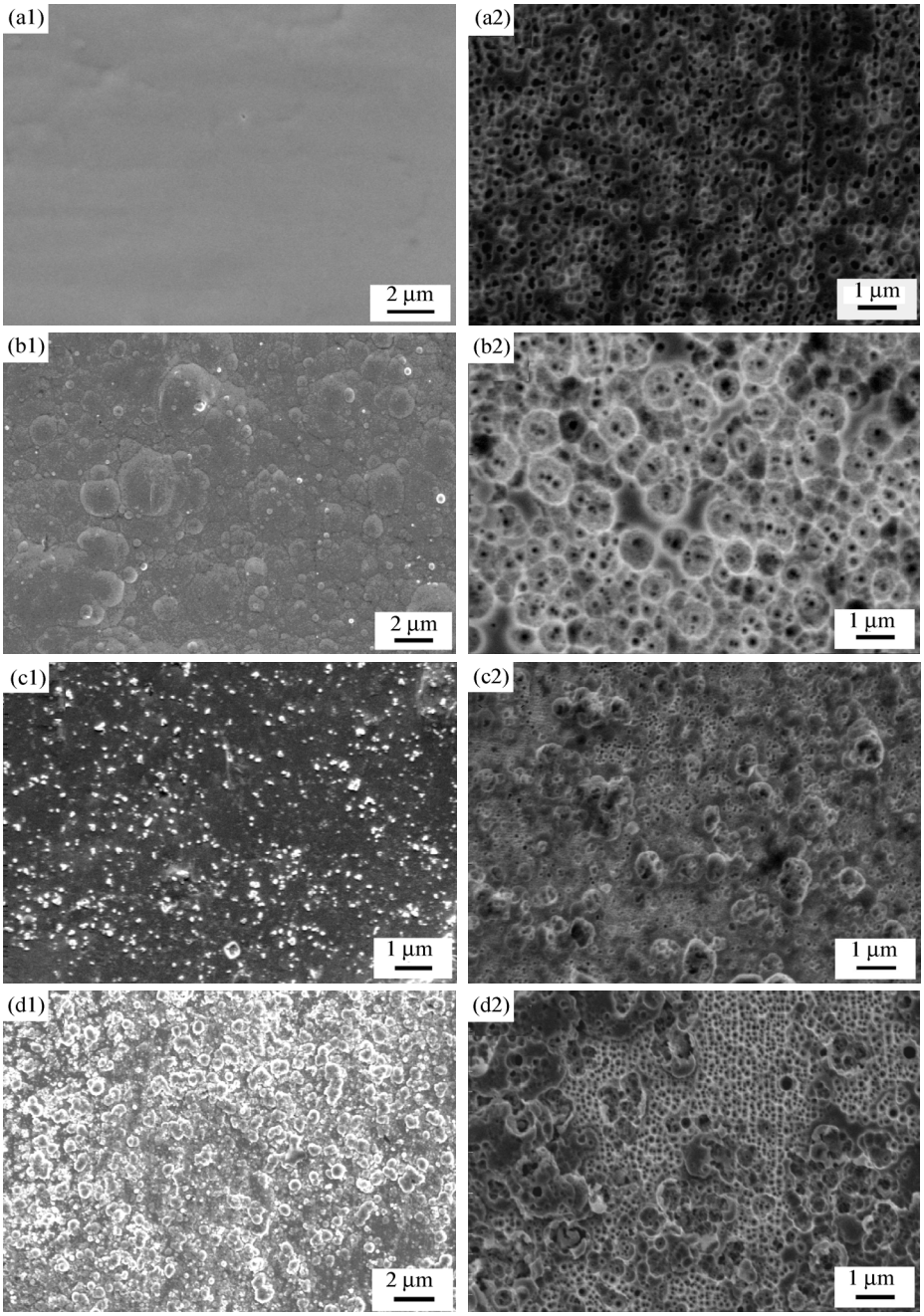

Fig.5. SEM micrographs of the surface of NiP/NiP-SiC deposits prepared with various concentrations of SiC particles: (a) without SiC; (b) 2 g/L SiC; (c) 5 g/L SiC; (d) 10 g/L SiC; the specimens were obtained before (1) and after 28 d of exposure in 3.5wt% NaCl solution (2).

Table 2. Elements and SiC contents of the specimens wt%

Specimen	Ni	P	SiC
NiP	87.72	12.28	—
NiP-SiC2	87.68	10.90	1.32
NiP-SiC5	86.29	10.64	3.07
NiP-SiC10	84.12	10.53	5.35

After immersion in 3.5wt% NaCl solution for 28 d, all the coatings had typical pit corrosion morphology. Pits on the coating NiP, NiP-SiC2, and NiP-SiC10 were dense, and most SiC particles fell off the NiP-SiC10 coating. While pits on the NiP-SiC5 coating were sparse and their radius was small, SiC parti-

cles still embedded in NiP alloys. The energy dispersive X-ray (EDX) analysis of the pure copper substrate covered with the NiP coating and the NiP-SiC coatings after exposition in the corroding medium (28 d) did not reveal any copper or copper compounds. Thus, these four coatings were sufficiently tight to effectively protect the copper basis in the experimental conditions.

3.3. Potentiodynamic measurements

Typical anodic potentiodynamic polarization curves of electrodeposited NiP/NiP-SiC composite coatings with different SiC contents, measured in 3.5wt% NaCl solution, are presented in Fig. 6. From Fig. 6, a typical passivation behavior can be clearly observed in the NiP-SiC2 and NiP-SiC5 coatings in which the electrode is anodically polarized to a more positive potential whereas the value of the corresponding current remains limited. In general, the corrosion resistance of any alloy depent on the ability to form a surface protective film. Considering the fact that the pH of 3.5wt% NaCl solution used was around 6.0. The most possible cathodic reaction of the dissolved oxygen according to Ref. [19] is

$$O_2 + 2H_2O + 4e \rightarrow 4OH^-. \quad (1)$$

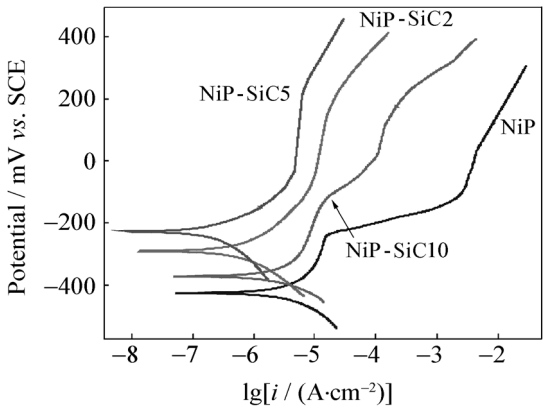

Fig. 6. Potentiodynamic polarization curves of as-plated electroplating NiP/NiP-SiC deposits in 3.5wt% NaCl solution in non-deaerated condition.

Hence, in non-deaerated condition, the reduction of the dissolved oxygen could give rise to an increase in pH closer to the coated surface. This led to insoluble corrosion products $Ni(OH)_2$ covering the coating surface. Moreover, the preferential dissolution of nickel led to the enrichment of phosphorus on the surface layer [20-22]. This enriched phosphorous reacted with water to form a layer of adsorbed hypophosphite anions ($H_2PO_2^-$). This layer in turn could block the supply of water to the electrode surface, thereby prevent the hydration of nickel. In the Fig. 6, with an increase of potential up to approximately 200 mV, the anodic current density dramatically increases with the increase of potential, indicating the breakdown of the above passive film and the occurrence of pitting corrosion in the NiP-SiC2 and NiP-SiC5 coatings.

The detailed electrochemical corrosion parameters are summarized in Table 3. As for the effect of SiC content on the passive behavior of the NiP and NiP-SiC composite coatings, as indicated in Table 3, a much wider passive range and lower passive current density are observed for the NiP-SiC5 coating when compared with the other composite coatings. It indicated that the NiP-SiC5 coating had a high density of nucleation sites for passive films, which led to high fraction of passive layers, and thus a lower passive current density. However, no obviously passive behavior occurred for the NiP and NiP-SiC10 coatings. By combining Fig. 6 and Table 3, it was clearly observed that the corrosion potential of the NiP-SiC coatings increased gradually from −422 to −224 mV with the increasing of SiC content from 0 to 3.07wt%. Moreover, the corrosion current density of the NiP-SiC coatings decreased gradually with the increasing of SiC content (0-3.07wt%), and the corrosion current density of the NiP-SiC5 coating was eleven times lower than that of the NiP coating. The NiP coating without obvious passive process had the highest corrosion current density, thus potentially the worst corrosion resistance compared with the NiP-SiC5 coating. Based on the above results, the introduction of proper SiC particles into the NiP coating would enhance the anticorrosive ability of the NiP coating for the attack of Cl^- and the best anticorrosion material should be the NiP-SiC5 coating.

3.4. Electrochemical impedance spectroscopy

The Nyquist impedance (Z) plots obtained for the NiP/NiP-SiC coatings after 28 d immersion in 3.5wt% NaCl solution, at the respective open circuit potentials, are shown in Fig. 7. The Nyquist plots of all the NiP and NiP-SiC composite coatings studied exhibit a single semicircle; however, the diameter of the semicircle is sharply increased with the gradual increasing of SiC content (from 0 to 3.07wt%), indicating that the NiP-SiC composite coatings have much a higher corrosion resistance. In addition, a diffusion-controlled charge transfer is observed at low frequency, as depicted in Fig. 7(b). Such a diffusion process may indicate that the corrosion mechanism of the NiP coating is controlled not only by a charge transfer step but also by the diffusion process.

To account for the corrosion behavior of the NiP-SiC coatings, an equivalent circuit model was proposed to simulate the metal/solution interface. The equivalent circuit model for the corrosion behavior of

the NiP-SiC coatings in the NaCl solution is shown in Fig. 8, where R_s is the solution resistance, C_{dl} is the double-layer capacitance, and R_{ct} is the charge-transfer resistance. The calculated equivalent circuit parameters for the NiP and NiP-SiC coatings with different SiC contents are presented in Table 4. After 28 d immersion in 3.5wt% NaCl solution, the corrosion of the NiP coating was a mixed-controlled electrode process, so it was decided to take a diffusion element into account in the calculations for these spectrums. Parameter W, connected in series with R_{ct} and in parallel with C_{dl}, was incorporated into the equivalent circuit diagram of the impedance spectrum of the NiP-SiC coating after 28 d of exposure.

Table 3. Corrosion potential (E_{corr}), corrosion current density (i_{corr}), passive current density (i_{pass}) and passive range (ΔE) of the NiP and NiP-SiC composite coatings with different SiC contents measured in 3.5wt% NaCl solution

Specimen	E_{corr} / mV	i_{corr} / (μA·cm^{-2})	i_{pass} / (μA·cm^{-2})	ΔE / mV
NiP	–422	8.7	—	—
NiP-SiC2	–289	1.8	11.1	204
NiP-SiC5	–224	0.8	4.7	252
NiP-SiC10	–369	5.8	—	—

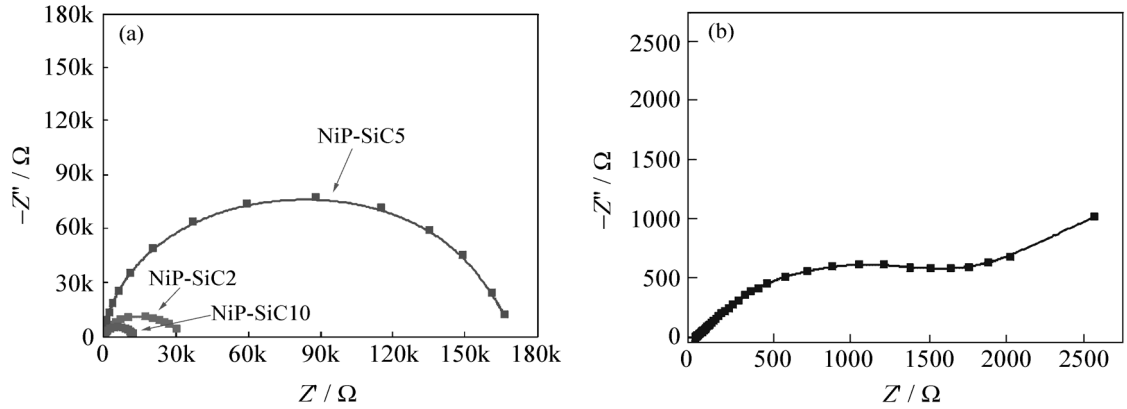

Fig. 7. Nyquist impedance diagrams registered after 28 d immersion in 3.5wt% NaCl solution: (a) NiP-SiC coatings; (b) NiP coating.

In Table 4, R_s was low and approximately constant, which should be a strong function of the distance between the tip of Luggin capillary and the coatings. The charge-transfer impedance increased with the gradual increasing of SiC content (from 0 to 3.07wt%) in the NiP-SiC coatings, which indicated the better corrosion resistance of the NiP-SiC5 coating. The double-layer capacitance decreased with the increasing of SiC content (from 0 to 3.07wt%), indicating the smooth and protective nature of the NiP-SiC5 coating [23].

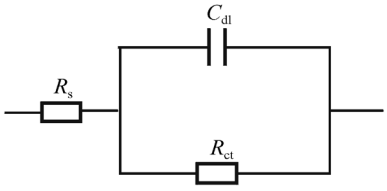

Fig. 8. Equivalent circuit model for the corrosion behavior of the NiP-SiC coatings in 3.5wt% NaCl solution.

Table 4. Equivalent circuit parameters determined by modeling the impedance spectra of NiP and NiP-SiC with different SiC contents after 28 d immersion in 3.5wt% NaCl solution

Specimen	R_s / (Ω·cm^2)	C_{dl} / (μF·cm^{-2})	R_{ct} / (kΩ·cm^2)	W / (Ω·cm^2·s$^{-1/2}$)	Error $\lvert Z\rvert$ / %
NiP	0.50	429.90	2.20	0.006	4.55
NiP-SiC2	0.53	60.11	31.49	—	2.10
NiP-SiC5	0.55	25.81	165.40	—	1.32
NiP-SiC10	0.51	60.18	11.48	—	1.28

3.5. Influence of nano-SiC particles on the corrosion characteristics of the NiP coating

All the above SEM observations, consistent with those electrochemical impedance spectra and evaluated by the polarization curves, further supported the conclusion that the corrosion resistance of the NiP-SiC coatings in NaCl solution increased with the increasing SiC content (from 0 to 3.07wt%) and then decreased with the content of SiC changing from 3.07wt% to 5.35wt%, and that the NiP-SiC5 coating exhibited the best protection against corrosive media.

The reasons that the corrosion resistance of

NiP-SiC coatings in NaCl solution increased with increasing SiC content (from 0 to 3.07wt%) were as follows: (1) nonconductive SiC particles were dispersed in coating uniformly, eliminated the exposed area of NiP coating, and shuffled the corrosion potential of coating; (2) passivation first started on the surface defects of coatings, and the NiP-SiC coatings had a high density of boundaries between nano-particles and the NiP matrix. Hence, it was believed that the NiP-SiC coatings had a high density of nucleation sites for passive films, which led to a high fraction of passive layer and low corrosion rate.

The main causes for the deterioration of corrosion resistance of the NiP-SiC composite coating when the concentration of nano-particles increased from 5 to 10 g/L were as follows: (1) with the increase of SiC particles in the composite coating, interface between metal matrix and particles enlarged, the discontinuous interface surrounded with particles had interspace, the agglomerates of particles led to uneven surface, and the particles had not been effectively covered by the NiP alloy; (2) a large amount of added SiC nano-particles wedged in and segmented the original passivated uniform coating, enlarging the interface area of the coating, increasing interface energy and increasing the number of corrosion microcells.

4. Conclusion

Amorphous NiP composite coatings with nano-sized SiC particles of different SiC contents are prepared by direct current electrodeposition process. The corrosion resistance gradually increases with the increasing SiC content from 0 to 3.07wt%, then decreases when the SiC content increased from 3.07wt% to 5.35wt%. Compared with the other deposits, the NiP-SiC5 coating has the best corrosion resistance. The corrosion resistance of the NiP-SiC5 coating is believed to be improved by the rapid formation of continuous Ni hydroxide passive films at surface defects and the relatively higher integrity of passive films as a result of the smooth and protective nature of passive films formed on the NiP-SiC5 coating. It shows the importance of taking into account not only the compound quantity of co-deposited particles but also the dispersion degree of particles when determining the composite properties.

References

[1] D.H. Jeong, U. Erb, K.T. Aust, *et al.*, The relationship between hardness and abrasive wear resistance of electrodeposited nanocrystalline Ni-P coatings, *Scripta. Mater.*, 48(2003), No.8, p.1067.

[2] Y.D. He, H.F. Fu, X.G. Lia, *et al.*, Microstructure and properties of mechanical attrition enhanced electroless Ni-P plating on magnesium alloy, *Scripta. Mater.*, 58(2008), No.6, p.504.

[3] J.N. Balaraju, T.S.N. Sankara Narayanan, and S.K. Seshadri, Electroless Ni-P composite coatings, *J. Appl. Electrochem.*, 33(2003), No.9, p.807.

[4] A. Grosjean, M. Rezrazi, J. Takadoum, *et al.*, Hardness, friction and wear characteristics of nickel-SiC electroless composite deposits, *Surf. Coat. Technol.*, 137(2001), No.1, p.92.

[5] M.R. Kalantary, K.A. Holbrook, and P.B. Wells, Optimization of a bath for electroless plating and its use for the production of nickel-phosphorus-silicon carbide coatings, *Trans. Inst. Met. Finish.*, 71(1993), No.2, p.55.

[6] N.V. Mandich and J.K. Dennis, Codeposition of nano-diamonds with chromium, *Met. Finish.*, 99(2001), No.6, p.117.

[7] M. Sarret, C. Müller, and A. Amell, Electroless NiP micro- and nano-composite coatings, *Surf. Coat. Technol.*, 201(2006), No.1-2, p.389.

[8] J.Q. Gao, L. Liu, Y.T. Wu, *et al.*, Electroless Ni-P-SiC composite coatings with superfine particles, *Surf. Coat. Technol.*, 200(2006), No.20-21, p.5836.

[9] X.H. Jie, X. Cheng, G.H. Lu, *et al.*, Slide wear behavior of Ni-P-SiC(nano) composite coating, *Heat Treat. Met.* (in Chinese), 32(2007), No.4, p.51.

[10] H.H. Kung, H.H. Wen, T.K. Shih, *et al.*, Ni-P-SiC composite produced by pulse and direct current plating, *Mater. Chem. Phys.*, 100(2006), No.1, p.54.

[11] C.J. Lin, K.C. Chen, and J.L. He, The cavitation erosion behavior of electroless Ni-P-SiC composite coating, *Wear*, 261(2006), No.11-12, p.1390.

[12] C.C. Min, D.G. Ming, T.K. Shih, *et al.*, The Ni-P-SiC composite produced by electro-codeposition, *Mater. Chem. Phys.*, 92(2005), No.1, p.146.

[13] C.F. Malfatti, H.M. Veit, T.L. Menezes, *et al.*, The surfactant addition effect in the elaboration of electrodepositated NiP-SiC composite coatings, *Surf. Coat. Technol.*, 201(2007), No.14, p.6318.

[14] Y.D. Chen, X.H. Jie, and G.H. Lu, Properties of brush plating Ni-P-Nano SiC composite coating, *Mater. Prot.* (in Chinese), 39(2006), No.3, p.11.

[15] C.F. Malfatti, F.J. Zoppas, C.B. Sontos, *et al.*, NiP/SiC composite coatings: the effects of particles on the electrochemical behaviour, *Corros. Sci.*, 47(2005), No.3, p.567.

[16] J. Li and B.Y. Jiang, Properties of electroless nickel alloy plating, *Corros. Prot.* (in Chinese), 26(2005), No.8, p.326.

[17] B.A. Boukamp, A linear Kronig-Kramers transform test for immittance date validation, *J. Electrochem. Soc.*, 142(1995), No.6, p.1885.

[18] M. Stern and A.L. Geary, Electrochemical polarization, Part 1: Theoretical analysis of the shape of polarization curves, *J. Electrochem. Soc.*, 104(1957), No.1, p.56.

[19] M.G. Fontana and N.D. Greene, *Corrosion Engineering*, McGraw-Hill Book Co., New York, 1967, p.10.

[20] J. Flis and D.J. Duquette, Effect of phosphorus on anodic dissolution and passivation of nickel in near-neutral solution, *Corrosion*, 41(1985), No.12, p.700.

[21] J.L. Carbajal and R.E. White, Electrochemical production

and corrosion testing of amorphous Ni-P, *J. Electrochem. Soc.*, 135(1988), No.12, p.2952.

[22] R.B. Diegle, N.R. Sorensen, C.R. Clayton, *et al.*, An XPS investigation into the passivity of an amorphous Ni-20P alloy, *J. Electrochem. Soc.*, 135(1988), No.5, p.1085.

[23] Kh.M.S. Youssef, C.C. Koch, and P.S. Fedkiw, Improved corrosion behavior of nanocrystalline zinc produced by pulse-current electrodeposition, *Corros. Sci.*, 46(2004), No.5, p.51.